

The Orbit of Asteroid 215188 (2000 NM)⁰

L. Jain¹, J. Li², M. Shapiro³, and A. Wang⁴

¹ Frisco Centennial High School, Frisco TX

² Newark Academy, Livingston NJ

³ Newton South High School, Newton MA
Email: mariel.shapiro@gmail.com
GitHub: <https://github.com/marielshapiro>

⁴ Aragon High School, San Mateo CA

August 6, 2022

ABSTRACT

In this study, we collected astrometric and photometric data on the near-Earth asteroid 2000 NM. We used these data to develop an orbit model of the asteroid and analyze the composition and size. As 2000 NM meets the definition of a potentially-hazardous asteroid, we evaluate the risk of future collision with Earth to contribute to the International Astronomical Union's Minor Planet Center Database(MPC). We find that the asteroid does indeed pose a risk of potential collision with Earth in the distant future. However, our results are limited due to weaknesses in the algorithm we employed. Additionally, our data represent only a small portion of the asteroid's orbit and further observation is required to model the entire orbit of 2000 NM.

1. Introduction

Asteroids and comets are integral to understanding the history and composition of our solar system. By observing these bodies, we can create models that estimate their size, shape, and composition. These models help us gain a better understanding of what the solar system was like during its early years. Models can also be used to measure the position of asteroids, and predict where they will be in the future. This becomes particularly important when the object of study is a near-Earth asteroid, an object whose orbit brings it into close proximity with Earth.

Our object of study, 2000 NM, is an Apollo asteroid: a class of near-Earth asteroids characterized by having a semi-major axis greater than that of Earth's and a perihelion distance less than Earth's aphelion distance (NASA Jet Propulsion Laboratory web archive). This means that 2000 NM's orbit intersects with Earth's orbit twice every period, making it essential to understand 2000 NM's behavior and composition. We investigate 2000 NM's orbit in this paper by constructing an orbit model, deducing our asteroid's orbital elements and chemical composition, and modeling our asteroid's rotation.

This paper is structured as follows: In Methods, we describe how we obtained our data and the techniques we used to analyze it; we report our results in Results; finally, we discuss the significance of our findings and conclude our paper in the Conclusion.

2. Methods

2.1. Observing Equipment and Data Collection

We accumulated data through observations using the 12-inch and 16-inch telescopes at the Leitner Observatory and the

iTelescope T5 in Mayhill New Mexico (iTelescope.net 2014).

To point the Leitner telescopes, we obtained an estimate for the Right Ascension and Declination at our observing time using the JPL Horizons Ephemeris Generator (NASA Jet Propulsion Lab 2022). Based on the position of our asteroid, we calibrated the telescope using one of the stars Zubenelgenubi, Zubenesh, or Arcturus, which were near the JPL values for right ascension and declination of 2000 NM. We took primarily 60-second exposures of our asteroid.

We used the luminance and empty filters on the 12-inch and 16-inch telescopes respectively to conduct astrometric observations. To obtain photometric data, we used the Sloan Green and Sloan Red filters on the 16-inch telescope. Figure 1 is an example of a 60 second exposure taken on the 16 inch telescope with an empty filter.

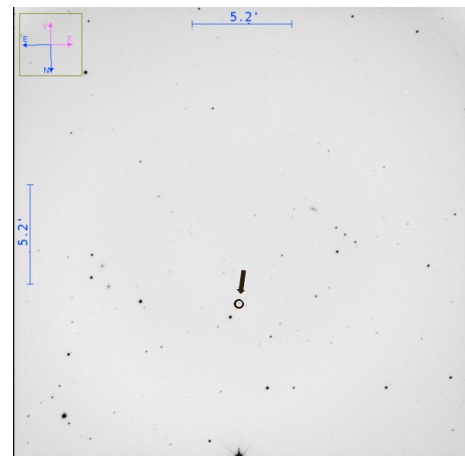


Fig. 1. CCD image of 2000 NM from the 16-inch telescope. 2000 NM is denoted with an arrow and colors are inverted for printing purposes

⁰ Authors contributed equally to this work and are listed alphabetically

On iTelescope T5, we used a slightly different procedure. We looked up the Right Ascension and Declination at the time of observation using JPL, and selected the filters and exposure times that the telescope would use to take images of our asteroid. We only had one successful night of observations on the T5 and took 30-second and 60-second exposures of our asteroid using the clear filter.

2.2. Data Processing

We began processing our data by removing all the images where our object was not visible due to clouds or poor focus. On the images where we could see our object, we ran the solve-field algorithm to attach the World Coordinate System (WCS). We also used the align, centroid, and screen stretch features of AstroImageJ to compile our photometric and astrometric data (Collins et al. 2017). This enabled us to extract the right ascension, declination, and flux of our Asteroid.

Photometry and Astrometry Data				
JD	RA	Dec	ApMag	Filter
2459764.609	15.744	-21.282	14.383	E
2459764.617	15.744	-21.279	14.412	E
2459768.576	15.598	-15.521	14.346	E
2459768.584	15.598	-15.508	14.466	E
2459768.591	15.598	-15.498	14.475	E
2459775.564	15.374	-4.090	14.828	L
2459775.571	15.374	-4.078	14.894	L
2459782.574	15.186	8.283	14.712	L
2459783.601	15.161	10.112	14.290	L
2459783.611	15.161	10.130	14.787	L
2459783.721	15.158	10.327	14.872	L
2459783.729	15.158	10.342	15.152	L
2459783.746	15.158	10.372	14.855	L
2459784.568	15.139	11.831	14.896	E
2459784.576	15.138	11.846	14.838	E
2459784.583	15.138	11.858	13.743	E
2459787.563	15.070	17.109	15.739	SG
2459787.569	15.070	17.118	15.753	SG
2459787.577	15.069	17.133	15.570	SG
2459787.579	15.069	17.137	15.019	SR
2459787.591	15.069	17.156	15.081	SR
2459789.555	15.025	20.556	15.295	E
2459789.563	15.025	20.569	15.313	E
2459791.606	14.980	24.036	16.055	E
2459791.614	14.980	24.048	15.913	E
2459791.628	14.979	24.072	16.241	SG
2459791.640	14.979	24.091	15.350	SR

Table 1. Data collected using the 16 inch, 12 inch and iTelescope T5 using filters E(empty), L(luminance), SG(Sloan Green), and SR(Sloan Red filters). The Julian Day, filter, and observed values for right ascension, declination, and apparent magnitude are listed.

We performed these techniques on one image out of every set of ten images for every night of data. After finding the flux of our asteroid(b_1, b_2), we found a calibration star near the asteroid. We found the calibration star's instrumental magnitude by inputting its right ascension and declination to the American Association for Variable Star Observers' Photometric All-Sky Survey(APASS), a sky survey that cataloged stars with their apparent magnitudes(M_1) (of Variable Star Observers Photometric All Sky Survey 2018). We used the following equation¹ to find

¹ (Faison 2016a)

the asteroid's apparent magnitude(M_2):

$$M_1 - M_2 = -2.5 \log\left(\frac{b_1}{b_2}\right) \quad (1)$$

2.3. Orbit Modeling

After collecting and processing the data, we had 27 data points of the right ascension and declination of our asteroid over nine nights (Table 1). In order to model the orbit of the asteroid over time, we implemented the Störmer Verlet integration method in which we modeled the motion of the asteroid as a result of the gravitational effects of significant perturbers in our solar system: the Sun, Jupiter, and, because this asteroid is near-Earth, the Earth and Moon. This method requires the position and velocity of the object at a certain time, from which the kinematics are modeled based on rates such as velocity and acceleration applied over small time increments. The goal was to use our Störmer Verlet numerical integrator to output position and velocity vectors for 2000 NM that are consistent with our observed values.

We utilized the Method of Laplace to determine a preliminary position and velocity at the starting time of the integration. We then employed a Monte Carlo genetic algorithm to create a "cloud" of 100 asteroids with varying positions and velocities described by a Gaussian distribution centered around the "parent" previous position and velocity. These asteroids were then integrated forward using the same Störmer Verlet method to determine which was most "fit" (had the least variation in topocentric right ascension and declination from our measured values) to be selected as the parent of the next generation of another 100 "offspring".

A major technical issue we faced was slow processing speeds, which was largely influenced by the time increment in the integration function. However, any time step that was larger than approximately 0.001 days would "jump" over consecutive data points. Thus, we had to incorporate an adaptive time increment that would be larger when the precision was not necessary (such as between days on which data was collected) and smaller in between times at which data was collected on the same day. In the end, our genetic algorithm was run for 115 adaptive generations stacked on top of a first non-adaptive generation

Another technical issue we faced was that the model would converge to a local minimum if the best model of initial generations was too far off(the models would progressively get better but gradually deviate from the globally best model). Because of this, we had to strike a balance in choosing the right standard deviation: if it was too high, the results would spread too far and fall into local minima, but if it was too low, it would not reach beyond the local minima. Figure 2 is an image of our orbit model visualization depicting 2000 NM relative to the Sun, Earth, Jupiter and Saturn.

2.4. Albedo and Diameter Calculation

To find the color index, we used a Sloan red exposure and a Sloan green exposure taken at similar times on the same night. Next, we used the centroid feature on AstroImageJ to find the right ascension, declination, and flux for the 30 reference stars on each image. We then calculated instrumental magnitude

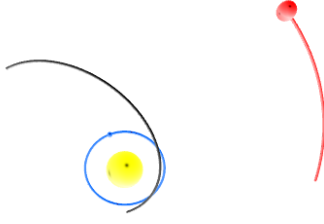


Fig. 2. Vpython visualization of our Störmer-Verlet integration method with the bodies that perturb the asteroid: the Sun, Earth, and Jupiter

using Equation 1.

Next, we used APASS to obtain a CSV file with the right ascension, declination, SG magnitude and SR magnitude for all the known stars in our field of view. We then wrote a program to match the reference stars we found to the APASS stars, and compiled a list of the absolute SR and SG magnitudes for the reference stars we found. After, we plotted the instrumental magnitude difference against the absolute magnitude difference and used least squares regression to calculate a line of best fit. Finally, we used the trendline with the measured instrumental magnitude difference for 2000 NM to find the color index. With this we used (Equation 2)² to calculate the phase angle and used it in (Equation 3)³ to calculate the absolute magnitude of 2000NM. We then used JPL and the albedo to estimate the diameter of the asteroid.

$$p = \frac{1 + \cos \beta}{2} \quad (2)$$

$$m = H + 5 \log D_E + 5 \log D_S - 2.5 \log p \quad (3)$$

p	fraction of object illuminated by the sun
β	phase angle
D_E	distance from Earth to Asteroid
D_S	distance from Sun to Asteroid
H	Absolute Magnitude of asteroid

2.5. Light Curve

Obtaining a light curve of 2000 NM can inform us of the rotational period of our asteroid (how fast our object rotates), which is significant in analyzing our asteroid's physical behavior.

We began by performing photometry and astrometry on the images from the luminance filter on July 30th. We chose to use images from this night for their clarity, focus, and minimal noise, which would reduce the uncertainty of the flux and the apparent magnitude.

We graphed the apparent magnitude versus the time, which we adjusted by setting our first observational time to 0 solar days

(Figure 3). Using the SciPy⁴ package, we used the Equation 4 to fit a curve to our data:

$$y = A \sin\left(\frac{2\pi}{T} + c\right) + h \quad (4)$$

We adjusted our amplitude, period, phase, and offset accordingly to improve the fit of the function. Amplitude, phase, and offset were determined visually, while the period was determined via calculation, as our data was taken over the span of approximately 1 hour (1/24 days).

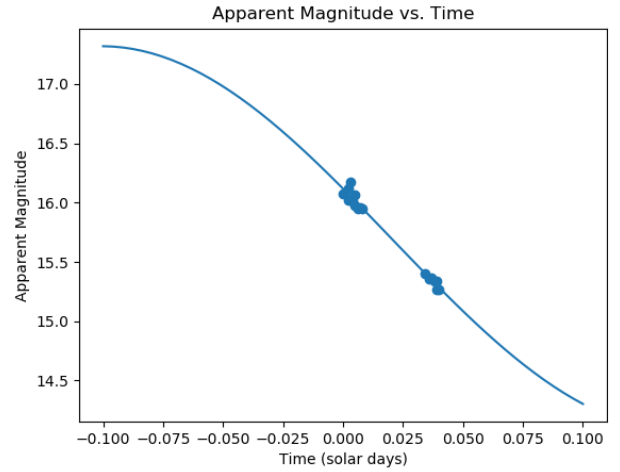


Fig. 3. Apparent Magnitude of 2000 NM over one observing night. A sinusoidal model is fit to the data to estimate the rotational period of the asteroid.

2.6. Long Term Prediction

In order to predict the long term orbit of 2000 NM, we used REBOUND, which is a complex N-body simulator which runs faster than Störmer-Verlet or Euler integration (Rein & Liu 2012). The main body that the asteroid orbited around was the Sun. In this simulation, we also assumed that the mass of the asteroid was negligible in comparison with the Sun. We also included the Earth-Moon Barycenter, Jupiter, and Saturn as perturbors to the asteroid's orbit. Then, using the initial position and velocity of our asteroid from our genetic algorithm, we predicted the closest approach distance of our asteroid over a hundred Gaussian years, through a time step of 0.001 Gaussian days. To set the uncertainty, we took the difference in time between the previous time step and the time step that included the closest approach distance.

3. Results

Table 2 shows the orbit model from Verlet integrator, Table 3 shows the osculating orbital elements, and Table 4 shows the results of the REBOUND integration.

² (Faison 2016b)

³ (Ford 2019)

⁴ (Virtanen et al. 2020)

Orbit Model		
	Calculated Values	Accepted Values
Position Vector	(6.558E+09, -1.708E+11, -7.535E+10)	(7.909e+09, -2.230e+11, -9.120e+10)
Velocity Vector	(2.275e9, 9.172E+08, 1.449E+09)	(8.1475e+09, 2.44543e+8, 7.01658e+09)

Table 2. Resulting position and velocity from our Verlet integrator. Vectors given for JD 2459764.5 at 00:00 UTC, units are meters(position) and meters/solar day(velocity). Accepted values come from JPL Horizons

Osculating Orbital Elements		
Orbital Element	Calculated Value	Accepted Value
a	0.622 AU	2.687 AU
e	0.999	0.622
i	17.402°	22.461°
q	1.624E-05 AU	0.903 AU
ω	0.850°	70.058°
Ω	-91.555°	-274.675°

Table 3. Values calculated using our numerical integrator for semimajor axis(a), eccentricity(e), inclination(e), perihelion(q), argument of perihelion(ω), and longitude of ascending node(Ω). Accepted values come from Minor Planet Center Database(International Astronomical Union 2022) and JPL Horizons

Using our Least Squares Regression line, we estimated a calibrated Apparent Magnitude (or Color index) to be 0.747. This color index corresponds to an S-type or siliceous asteroid. These asteroids generally have an albedo of about 0.2 and are usually composed of silicates and nickel iron (Zolensky et al. 2018). We could not find previously determined values for Albedo and Color index of 2000 NM from JPL or MPC and were thus unable to determine if our results were consistent with accepted values.

Using Equations 2 and 3, we calculated the Absolute Magnitude of 2000 NM to be 13.60, this is consistent with the accepted JPL value of 15.53. We then calculated the diameter of the asteroid to be about 5.7 km using the Asteroid Size Estimator.

REBOUND Integration	
	Calculated Value
Closes Approach Time	125.1574904 GD
Closest Approach Distance	0.0019075423595 AU
Uncertainty	8.399251271384855e-05 GD

Table 4. Results from REBOUND N-Body Numerical Integrator(Rein & Liu 2012)

4. Conclusion

The goal of this project was to model the orbit of the near-Earth asteroid 2000 NM and study its characteristics. The eccentricity, inclination and period we estimated from our model were largely consistent with accepted JPL values. Additionally, the position and velocity vectors derived from our numerical integrator were mostly within the same order of

magnitude as the JPL Horizons ephemeris. We could not find previously determined values for Albedo and Color index of 2000 NM from JPL or the Minor Planet Center Database and thus were unable to determine if our results were consistent with accepted values. Other values and properties determined from our algorithm, including semi major axis, perihelion distance, and longitude of ascending node, differed greatly from our astrometric observations and accepted values. There are several potential causes of these discrepancies which we will address in the following paragraphs.

A limitation we found with our Laplace method was that it has to approximate whenever the time step is not uniform. While we could have tried to take a weighted average of positions or velocities, it still would not have negated all of the error. One issue we encountered with the genetic algorithm is the computing power required to run a large number of generations with a large number of offspring. After running our genetic algorithm over multiple hours, the standard deviation of our model had not fully converged. To account for this in the future we would allocate more time to run the algorithm for more accurate results.

Another approximation we made was using the Earth-Moon Barycenter instead of a geocentric or topocentric Earth vector. While we could have separated the Earth and Moon from the Earth and Moon barycenter in the REBOUND simulator, the change in position would be five orders of magnitude less than the closest approach distance. In REBOUND, we also tried to propagate a cloud of asteroids over a long period of time using the standard deviation from the genetic algorithm. We hoped to determine how the error bars changed over the long-term orbit, but we were again limited by our computing power and were unable to run the cloud over a long-enough period of time.

Additionally, the Stormer Verlet numerical integration method may not be optimal to model the orbit of 2000 NM. In the algorithm, only position is propagated and not velocity. Consequently, our resultant velocity was not very accurate as the model had not yet converged.

Also, our data were only collected during a small portion of the orbit, so extrapolating to the entire orbit is inaccurate. The relatively high period of rotation further limits our accuracy as we extrapolated 75 minutes of data to an orbital period of 11 hours. We would have benefited from having more observing sessions where we could collect a high volume of exposures.

Acknowledgements. We would like to thank the staff of the Yale Summer Program in Astrophysics for all of their support: Dr. Michael Faison for his wonderfully engaging lectures, Mr. Michael Warrenner for guiding our practice, Elijah, Hanna, and Julia for helping out no matter the time, and Ms. Kimberly Nucifora for all of the support.

References

- Collins, K. A., Kielkopf, J. F., Stassun, K. G., & Hessman, F. V. 2017, *The Astronomical Journal*, 153, 77
Faison, M. 2016a, *Method of Laplace Handout*, unpublished
Faison, M. 2016b, *Numerical Integration Handout*, unpublished
Ford, D. 2019, https://in-the-sky.org/article.php?term=absolute_magnitude
International Astronomical Union. 2022, *Minor Planet Center Database*, <https://minorplanetcenter.net>
iTelescope.net. 2014, <https://support.itlescope.net/support/solutions/articles/231902-telescope-5>

NASA Jet Propulsion Lab. 2022, JPLHorizons, <https://ssd.jpl.nasa.gov/horizons/app.html#/>
NASA Jet Propulsion Laboratory. web archive, <https://web.archive.org/web/20020202160655/http://neo.jpl.nasa.gov/neo/groups.html>
of Variable Star Observers Photometric All Sky Survey, A. A. 2018, <https://www.aavso.org/apass>
Rein, H. & Liu, S.-F. 2012, *Astronomy & Astrophysics*, 537, A128
Virtanen, P., Gommers, R., Oliphant, T. E., et al. 2020, *Nature Methods*, 17, 261
Zolensky, M. E., Abreu, N. M., Velbel, M. A., et al. 2018, in *Primitive Meteorites and Asteroids*, ed. N. Abreu (Elsevier), 59–204